

SUB-20 KHz LOW FREQUENCY NOISE NEAR ULTRAVIOLET MINIATURE EXTERNAL CAVITY LASER DIODE: SUPPLEMENTAL DOCUMENT

1. Laser diode epitaxial structure

The laser diode (LD) used in this study has a conventional GaN-based Fabry-Perot geometry. The epitaxial structure was grown in the Laboratory of Advanced Semiconductors for Photonics and Electronics (LASPE) of EPFL by metalorganic vapor phase epitaxy. The layer sequence of the diode is shown in Fig. S1.

The active layer consists of two 4-nm-thick InGaN quantum wells separated by a 10-nm-thick GaN barrier. The composition of these layers has been set to get laser emission at an approximate wavelength of 400 nm. The surrounding AlGaIn-layers ensure the vertical confinement of the emitting light by playing the role of cladding. The AlGaIn:Mg-based electron blocking layer (EBL) is introduced to avoid an overflow of electrons on the p-type side to compensate for the lower hole mobility.



Fig. S1 : Epitaxial structure of the laser diode.

2. Simulation of Fiber Bragg grating transmission

Requirements

To obtain a single-mode optical feedback on the laser diode, the Bragg wavelength of the fiber Bragg grating (FBG) has to be centered at the emission wavelength of the bare laser diode, which occurs around 400 nm. Then, the full width at half-maximum (FWHM) of the filter must be narrower than the free spectral range (FSR) of the diode cavity (26 pm) in order to lock the emission onto a unique mode. Finally, the maximum reflection of the FBG has to be sufficiently high to obtain the desired optical feedback. Here, the reflectivity coefficient (R) has been fixed at ~50% as it is a good compromise between the strength of the optical feedback and the available outcoupled power.

For a uniform grating, the reflection coefficient is given by [1]:

$$r = -\frac{i\kappa \sinh(\gamma L)}{\gamma \cosh(\gamma L) + i\Delta\beta \sinh(\gamma L)} \quad \#(1),$$

where $\gamma^2 = \kappa^2 - \Delta\beta^2$ and $\Delta\beta = \beta - \beta_0 = 2\pi\left(\frac{n_{eff}(\lambda_B)}{\lambda_B} - \frac{n_{eff}(\lambda)}{\lambda}\right)$

The Bragg propagation constant is $\beta_0 = \frac{2\pi}{\lambda_B}n_{eff}$ and the coupling coefficient is expressed by $\kappa = \frac{\pi\Delta n}{\lambda_B}$ where λ_B is the Bragg resonance wavelength, n_{eff} is the effective optical index and Δn is the amplitude of the effective index modulation imprinted during the Bragg photoinscription in the fiber. The Bragg wavelength also defines the grating period Λ following $\lambda_B = 2 * n_{eff} * \Lambda$.

The condition of resonance is reached for $\lambda = \lambda_B$, which is equivalent to $\Delta\beta = 0$. It implies that $r = -i \tanh(\kappa L)$, $R_{max} = r^2 = \tanh^2(\kappa L)$ and the transmission coefficient is given by $T = 1 - R$.

To simulate the theoretical response of a uniform fiber Bragg grating, only some parameters are required like the Bragg wavelength, the effective index n_{eff} of the modes in the grating, the index modulation Δn and the length of the grating L . The fiber properties determine the mean effective index, but the other parameters are linked to the fabrication of the component. From these data we can calculate κ , β , γ and finally R and T .

Index modulation and Bragg wavelength settings

The reflection bandwidth (FWHM) mainly depends on the length of the FBG. The longer the grating, the narrower it is. The amplitude of the index modulation affects the bandwidth to a lesser extent. In practice, when the grating is too long, a phase noise is introduced in the index modulation during the inscription, which will subsequently limit the minimal achievable bandwidth. The Bragg wavelength is determined by the effective index of the mode and the period of the grating. This period corresponds to the pitch of the interference field projected onto the fiber and is a function of the mutual angle between the two interfering writing beams of the Talbot interferometer.

Parameters impact on the performances

If the peak reflectivity of the FBG is set, the FWHM of the filter can be simulated for any length. The coupling coefficient is then used as an adjustment variable. One can find below in Fig. S2 the spectral transmission of the grating for three different lengths. The parameters used for the simulation are:

- $n_{eff} = 1.47348$.
- $\Delta n = 1.2 \times 10^{-4}$ ($L = 1 \text{ mm}$), 0.6×10^{-4} ($L = 2 \text{ mm}$), 0.4×10^{-4} ($L = 3 \text{ mm}$)
- $\Lambda = 135.61 \text{ nm}$

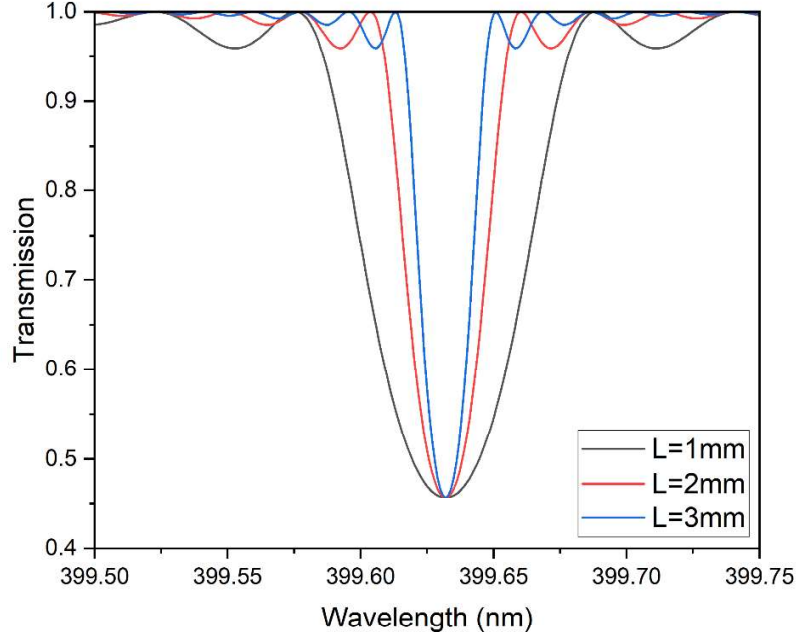


Fig. S2 : Simulated FBG transmission spectra for three different lengths. Simulation parameters are the following ones: $L=1\text{mm}$ / $\Delta n=1.2 \times 10^{-4}$ (black curve), $L=2\text{mm}$ / $\Delta n=0.6 \times 10^{-4}$ (red curve) and $L=3\text{mm}$ / $\Delta n=0.4 \times 10^{-4}$ (blue curve).

Final design

From the different simulations and the optical fiber properties, the length fulfilling the filtering requirements is 3 mm. A comparative graph between the optimum simulated result and the experiment is shown in Fig. S3.

We can then deduce:

- $\lambda_B = 2 \cdot n_{eff} \cdot \Lambda = 399,64 \text{ nm}$
- $\kappa = \frac{\pi \Delta n}{\lambda_B} = 322 \text{ m}^{-1}$
- $R_{max} = \tanh^2(\kappa L) = 0.558 = 55.8\%$
- $\text{FWHM} = 20 \text{ pm}$

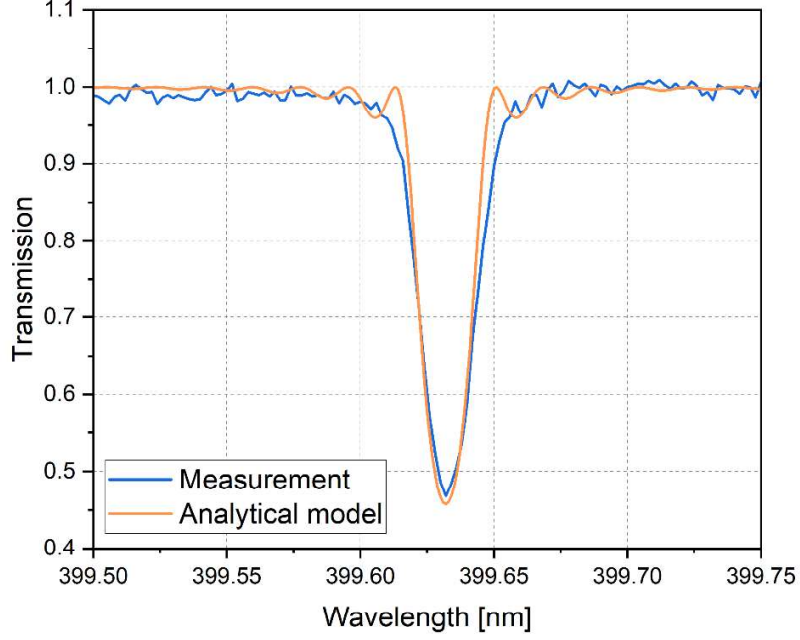


Fig. S3 : FBG transmission measurement (blue curve) and corresponding simulated spectrum (orange curve). The measured reflection is close to the simulated one. Simulation parameters are the following ones: FBG length = 3 mm, index modulation $\Delta n = 0.40 \times 10^{-4}$.

3. Output power versus side mode suppression ratio

Thanks to the simultaneous measurements of the optical power and the optical spectrum, the optimum tradeoff between power and side-mode suppression ratio (SMSR) can be determined. Fig. S4 displays the evolution of the optical power versus pump current with a saw tooth behavior that is common for such external cavity laser diode [2]. SMSR evolution versus pump current is also plotted. The SMSR shows an opposite slope sign compared with the optical power. Indeed, at the beginning of sequence 1 (see Fig. S4), the Bragg wavelength and the LD optical mode are overlapping each other leading to an optimum filtering effect. This results in a lower optical output power but an optimized SMSR. On the contrary, at the end of sequence 1, a poor wavelength overlap between the Bragg wavelength and the redshifted LD mode implies a degraded filtering effect, which leads to a larger output power at the expense of a reduced SMSR. The results shown in the main text are obtained for a pump current of 124 mA.

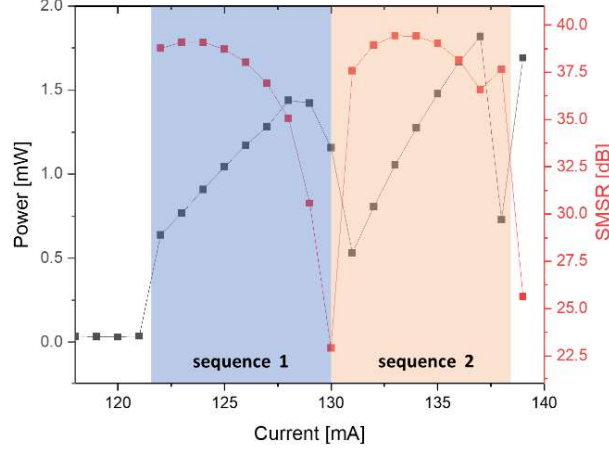


Fig. S4 : Output optical power and SMSR of the fiber Bragg grating laser (FGL) as a function of driving current

4. Retrieving the optical spectrum from frequency noise measurements

The objective of this appendix is to provide some insights into the link between the power spectral density (PSD) of the laser frequency noise $S_{\delta\nu}(f)$ and the optical spectrum $I_E(\nu)$. A more detailed explanation can be found in Refs. [3]–[6]. Let us consider the laser field $E(t)$ for which only phase fluctuations are taken into account:

$$E(t) = E_0 e^{i(2\pi\nu_0 t + \phi(t))},$$

where t is the time, E_0 is the amplitude of the laser field, ν_0 is the field mean frequency and $\phi(t)$ is the time-dependent phase. The optical spectrum $I_E(\nu)$ is the Fourier transform of the temporal autocorrelation of the laser field $R_E(\tau)$:

$$I_E(\nu) = \int_{-\infty}^{+\infty} R_E(\tau) e^{-i2\pi\nu\tau} d\tau. \#(2)$$

For a Gaussian noise $\phi(t)$, $R_E(\tau)$ can be written as:

$$R_E(\tau) = \langle E^*(t) E(t + \tau) \rangle ,$$

or in an expanded form:

$$R_E(\tau) = E_0^2 e^{i2\pi\nu_0\tau} e^{-\frac{1}{2}\langle [\phi(t+\tau) - \phi(t)]^2 \rangle}. \#(3)$$

The link between $\langle [\phi(t + \tau) - \phi(t)]^2 \rangle$ and the temporal correlation of the frequency noise $R_{\delta\nu}(\tau)$ is not trivial but a complete explanation can be found in Ref. [3]:

$$\langle [\phi(t + \tau) - \phi(t)]^2 \rangle \geq 2 \int_0^\tau (t - \tau) R_{\delta\nu}(\tau) dt. \#(4)$$

The main outcome of this treatment is to keep in mind that the temporal correlation of the frequency noise $R_{\delta\nu}(\tau)$ is linked to the laser noise PSD $S_{\delta\nu}(f)$, where f is the Fourier frequency, by the Wiener–Khinchine theorem:

$$R_{\delta\nu}(\tau) = \int_0^\infty S_{\delta\nu}(f) \cos(2\pi f t) df. \#(5)$$

Combining equations (4) and (5) leads to:

$$\langle [\phi(t + \tau) - \phi(t)]^2 \rangle \geq 2 \int_0^\infty S_{\delta\nu}(f) \int_0^\tau (t - \tau) \cos(2\pi f t) dt df, \#(6)$$

which allows to recast the expression of the temporal autocorrelation of the laser field in the following form:

$$R_E(\tau) = E_0^2 e^{i2\pi\nu_0\tau} \exp \left[-2 \int_0^\infty S_{\delta\nu}(f) \frac{\sin^2(\pi f \tau)}{f^2} df \right]. \#(7)$$

Finally, from Eq. (1), the relation between the PSD of the laser noise and the optical spectrum $I_E(\nu)$ can be described by the following relation, called the Elliott Formula [3]:

$$I_E(\nu) = E_0^2 \int_{-\infty}^{+\infty} e^{-i2\pi\nu\tau} e^{i2\pi\nu_0\tau} \exp \left[-2 \int_0^\infty S_{\delta\nu}(f) \frac{\sin^2(\pi f \tau)}{f^2} df \right] d\tau. \#(8)$$

From white frequency noise to Lorentzian profile

Considering a laser frequency noise (FN) only determined by spontaneous emission noise, then the FN is described by a white noise PSD $S_{\delta\nu}(f) = h_0$ (see Fig. S5 a)). Then the Elliott formula expressed by Eq. (8) reduces to:

$$I_E(\nu) = E_0^2 \int_{-\infty}^{+\infty} e^{i2\pi\tau(\nu_0 - \nu)} e^{-\pi^2 h_0 \tau^2} d\tau,$$

which can be recast into a Lorentzian function:

$$I_E(\nu) = E_0^2 \frac{h_0}{(\pi h_0/2)^2 + (\nu_0 - \nu)^2},$$

with a linewidth $\Delta\nu_{wn} = \pi h_0$.

As an illustration, for the white noise of our UV FGL shown in Fig. S5, we have $h_0 = 4149 \text{ Hz}^2/\text{Hz}$, the Lorentzian function is depicted by the yellow dashed line in Fig. S5.

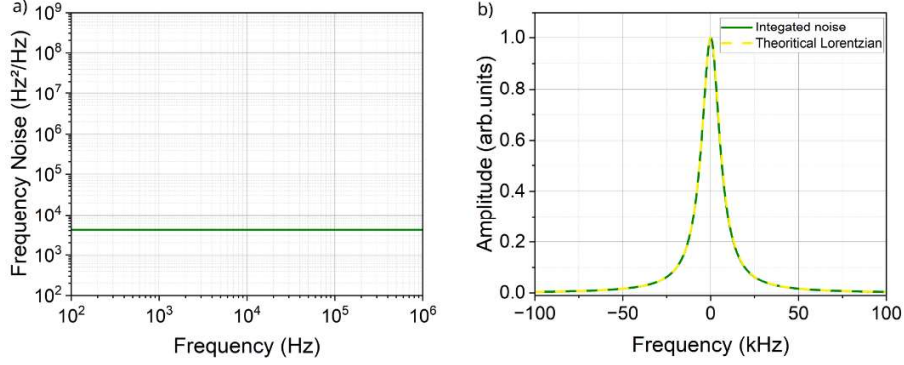


Fig. S5 : a) PSD of a frequency white noise $h_0 = 4149 \text{ Hz}^2/\text{Hz}$. b) Comparison between the integrated white noise deduced from the Elliott formula (green curve) and the analytical expression (yellow dashed line).

We can also perform a numerical integration of the white noise h_0 using Eq. (7) between 100 Hz and 1 MHz and see that the numerical integration overlaps well with the theoretical curve.

From flicker frequency noise to Gaussian profile

The case of a flicker noise ($S_{\delta\nu}(f) = h_1/f$) is not as straightforward as for the white noise, and gives the following form for the optical spectrum:

$$I_E(\nu) = E_0^2 \int_{-\infty}^{+\infty} e^{-i2\pi\nu\tau} e^{i2\pi\nu_0\tau} \exp \left[-2h_1 \int_0^\infty \frac{\sin^2(\pi f\tau)}{f^3} df \right] d\tau.$$

The problem faced is that the integral $\int_0^\infty \frac{\sin^2(\pi f\tau)}{f^3} df$ is not convergent. To circumvent this issue, and hence obtain a physically relevant result, we take advantage of the fact that the observation time is not infinite. Defining an appropriate observation time, and thus a lower bound to the frequency integration, leads to a Gaussian profile for the integrated optical spectrum [4]:

$$I_E(\omega) = E_0^2 \frac{\sqrt{\pi}}{\sigma} e^{-(\omega_0 - \omega)^2 / \sigma^2},$$

with ω the angular frequency, ω_0 the mean angular frequency of the laser and $\sigma^2 = 3.56h_1$.

Relation between frequency noise and optical spectrum

In the present experimental case, our FGL does exhibit a more complex noise PSD, so that no analytical formulas are applicable. However, we can perform a numerical integration on the measurement frequency bandwidth of Eq. (7). The resulting curve is plotted in Fig. S6. From this curve, the integrated laser linewidth can be extracted: $\Delta\nu = 720 \pm 120 \text{ kHz}$. For

comparison, the Beta line method [5] can also be used to assess the linewidth of the laser, and a similar value of 710 ± 120 kHz is obtained.

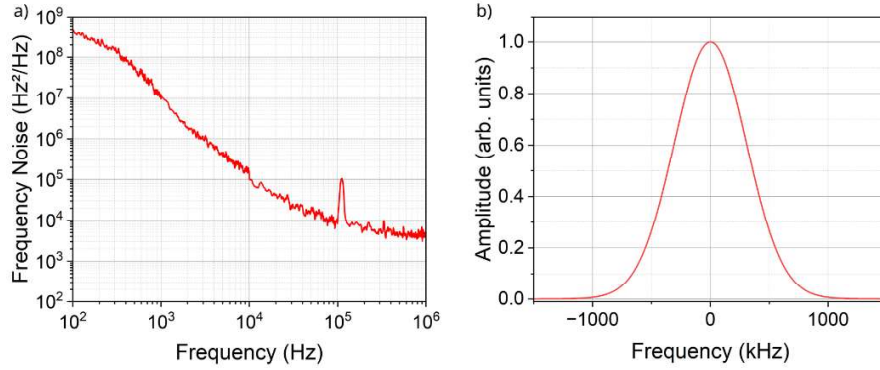


Fig. S6 : a) PSD of the frequency noise of the UV FGL. b) Integrated frequency noise deduced from the Elliott formula leading to a linewidth of 720 kHz.

References

1. R. Kashyap, Fiber Bragg Gratings, 2nd ed. (Academic Press, New York, 2009).
2. R. Lang and K. Kobayashi, "External optical feedback effects on semiconductor injection laser properties", IEEE J. Quantum Electron. **16**, 347-355 (1980).
3. D. S. Elliott, R. Roy, and S. J. Smith, "Extracavity laser band-shape and bandwidth modification", Phys. Rev. A **26**, 12-18 (1982).
4. G. M. Stéphan, T. T. Tam, S. Blin, *et al.*, "Laser line shape and spectral density of frequency noise", Phys. Rev. A **71**, 043809 (2005).
5. G. Di Domenico, S. Schilt, and P. Thomann, "Simple approach to the relation between laser frequency noise and laser line shape", Appl. Opt. **49**, 4801-4807 (2010).
6. K. Kikuchi, "Effect of 1/f-type FM noise on semiconductor-laser linewidth residual in high-power limit", IEEE J. Quantum Electron. **25**, 684-688 (1989).